Ultrafast Manipulation of Strong Coupling in Metal–Molecular Aggregate Hybrid Nanostructures

P. Vasa,[†] R. Pomraenke,[†] G. Cirmi,[‡] E. De Re,[‡] W. Wang,[†] S. Schwieger,[§] D. Leipold,[§] E. Runge,[§] G. Cerullo,[‡] and C. Lienau[†,*]

[†]Institut für Physik, Carl von Ossietzky Universität Oldenburg, Germany, [‡]IFN-CNR, Dipartimento di Fisica, Politecnico di Milano, Milano, Italy, and [§]Institut für Physik and Institut für Mikro- und Nanotechnologien, Technische Universität Ilmenau, Germany

ABSTRACT We demonstrate an ultrafast manipulation of the Rabi splitting energy Ω_R in a metal–molecular aggregate hybrid nanostructure. Femtosecond excitation drastically alters the optical properties of a model system formed by coating a gold nanoslit array with a thin J-aggregated dye layer. Controlled and reversible transient switching from strong ($\Omega_R \simeq 55$ meV) to weak ($\Omega_R \approx 0$) coupling on a sub-ps time scale is directly evidenced by mapping the nonequilibrium dispersion relations of the coupled excitations. Such a strong, externally controllable coupling of excitons and surface plasmon polaritons is of considerable interest for ultrafast all-optical switching applications in nanoscale plasmonic circuits.

KEYWORDS: surface plasmon polaritons · metal nanostructures · molecular aggregates · organic semiconductors · time-resolved spectroscopy

Future nanoplasmonic devices will most likely rely on the interplay between the strong intrinsic optical nonlinearities of excitonic nanostructures and the ability of metallic nano-objects to concentrate electromagnetic fields locally. Consequently, the optical properties of hybrid nanostructures comprising active materials, for example, semiconductors or J-aggregated molecules, and metals are currently attracting considerable attention.[1,2] In favorable geometries, these properties are governed by a new class of short-lived quasiparticles, exciton–surface plasmon polaritons, in short "excimons",[3] with hitherto unexplored nonequilibrium dynamics.[4] Their stationary, quasi-equilibrium properties have now been studied in a variety of rather different hybrid nanostructures, ranging from J-aggregated dye[5−8] or semiconductor quantum dots[9] deposited on thin metallic films to gold gratings on semiconductor quantum wells.[10] Excimons bear some similarities with mesoscopic microcavity polaritons, which are formed when semiconductor nanostructures are placed inside a dielectric resonator[11−14] and have found unique applications in, for example, polariton lasing[15,16] and condensation.[17,18] However, excimons can be spatially confined to tens of nm, whereas the characteristic length of microcavity polaritons is given by the optical wavelength.

The binding energy of such excimon quasiparticles, that is, their Rabi splitting energy $\Omega_R = \int \vec{\mu}_X(\vec{r}) \cdot \vec{E}_{SPP} dV$, is essentially given by the spatial overlap integral of the excitonic transition dipole moment density $\vec{\mu}_X(\vec{r})$ and the electric field vector $\vec{E}_{SPP}(\vec{r})$ of the local surface plasmon polariton (SPP) mode. Large Ω_R of up to several hundreds of meV have been demonstrated so far.[6−9,19] This necessarily implies that the optical properties of such strongly coupled hybrid structures can be drastically altered by externally manipulating $\vec{\mu}_X(\vec{r})$ or $\vec{E}_{SPP}(\vec{r})$. Due to the anticipated short quasiparticle lifetimes, such a control may occur on an extremely fast time scale and hence prove interesting, for example, for applications to ultrafast all-optical switching devices[20−22] with potentially nanometric size and single photon operation capability.[23]

In this manuscript, we report angle-resolved, ultrafast nonlinear optical spectra of a prototypical hybrid structure consisting of a gold nanoslit array coated with a J-aggregated dye film (Figure 1). We demonstrate transient, reversible, and essentially complete switching of Ω_R on a femtosecond time scale by manipulating the exciton dipole moment. Controlling the Ω_R results in pronounced, ultrafast changes of the sample reflectivity up to 40% at certain resonance wavelengths, making such a hybrid structure an externally switchable metallic mirror.

*Address correspondence to christoph.lienau@uni-oldenburg.de.

Received for review August 10, 2010 and accepted November 04, 2010.

Published online November 17, 2010.
10.1021/nn101973p

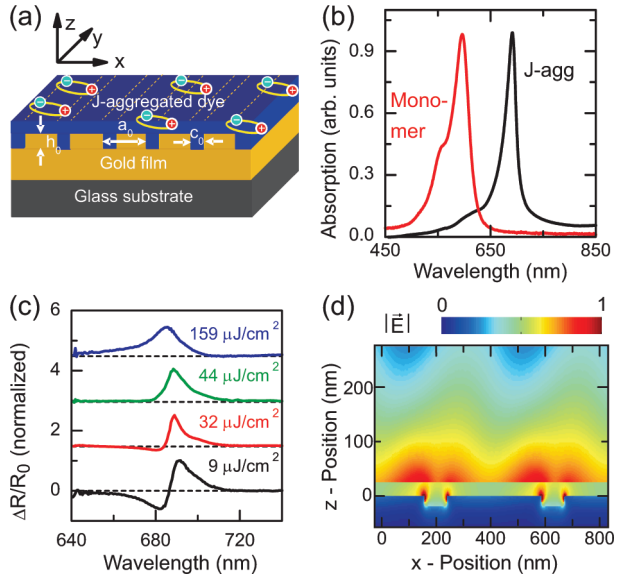

Figure 1. (a) Schematic of the metal−molecular aggregate hybrid nanostructure consisting of a 50 nm thick J-aggregate film spin-coated onto a gold nanoslit array with a_0 = 430 nm period, h_0 = 30 nm depth, and c_0 = 45 nm slit width. The dye-film thickness is measured from the top of the grating. (b) Room temperature absorption spectra of the cyanine dye in monomer (red) and J-aggregated (black) form. (c) Normalized $\Delta R/R_0$ spectra of the J-aggregated cyanine dye (T = 77 K) as a function of pump fluence (shifted for clarity as indicated by the dotted lines). (d) The calculated spatial distribution of the electric field amplitude $|\tilde{E}|$ for p-polarized excitation at 695 nm at the exciton−SPP crossing (θ = 32°) is characterized by a strong field enhancement in and near the slits as well as a discontinuity at the air−film interface.

SAMPLE FABRICATION

We investigate a hybrid nanostructure consisting of a 50 nm thick J-aggregated dye layer spin-coated onto a periodic array of nanoslits in a gold film, schematically shown in Figure 1a. The gold reflection gratings with a size of 150 × 150 μm^2 were fabricated by focused ion beam milling of periodic nanoslit arrays with different periods a_0 = 380−430 nm, depth h_0 = 30 nm, and slit width c_0 = 45 nm. The cyanine dye 2,2′-dimethyl-8-phenyl-5,6,5′,6′-dibenzothiacarbocyanine chloride (Hayashibara Biochemicals Laboratories, Inc.) is dissolved in a solution containing polyvinyl alcohol (PVA), water, and methanol. At a concentration of ~0.5 mols per dm^3 in dry PVA, the dye shows strong so-called J-aggregation.[24] This is evidenced by spectral narrowing of the optical absorption spectrum and a redshift of about 100 nm relative to the monomer spectrum to ~695 nm [Figure 1b]. The occurrence of this strong J-band in the absorption spectrum is generally attributed to the collective response of partially ordered domains containing ~10 optically coupled molecules.[24−26] A typical optical density of a 50 nm thick spin-coated film is ~0.4. This corresponds to a maximum excitonic absorption coefficient of $\alpha \sim 2 \times 10^5$ cm^{-1}, which is about 1 order of magnitude larger than that of a comparable film containing dye monomers. Their large absorption coefficients obviously make J-aggregates interesting candidates for studying exciton−SPP interactions.[5−7,13,14,19,27,28]

OPTICAL RESPONSE OF THE J-AGGREGATES

When spin-coated onto a planar gold film, the dye reduces the high reflectivity R_g of the gold film from more than 0.95 to less than 0.25 at the exciton resonance (see Supporting Information). Because the reflectivity spectrum of the bare gold film is unstructured, the measured signal is equivalent to a double-pass transmission through the dye film. Qualitatively, the planar dye film reflectivity spectrum $R_d = R_g - b \cdot L$ is rather well described by modeling the dye absorption by a single Lorentzian line shape $L(\omega) = (\gamma/\pi)/[(\omega - \omega_0)^2 + \gamma^2]$, centered at the exciton resonance with a width γ of only about 20 meV (8.5 nm) and a fluence-dependent amplitude b. Such a model, although found to describe well the results presented in this work, is certainly only approximate as it neglects disorder effects, known to be important for J-aggregated dye films.

Measurements of the nonlinear optical response of such a J-aggregated film deposited on a flat gold mirror are shown in Figure 1c. The figure displays ultrafast differential reflectivity $\Delta R/R_0 = (R - R_0)/R_0$ (R and R_0: reflected probe laser power in the presence and absence of the pump, respectively) spectra recorded under excitation at 620 nm, at a fixed pump−probe delay Δt = 150 fs and for various pump fluences F_{pu}. All spectra show an increase in reflectivity, $\Delta R > 0$, at the J-aggregate exciton resonance with its amplitude initially increasing linearly with F_{pu} (not shown). The off-resonant pump generates a transient increase in exciton population n_X. This results in a saturation of the exciton absorption $\alpha = \alpha_0 \cdot (1 - n_X)$ (α_0: absorption coefficient in the absence of pump) and, hence, an increase in intensity of the probe laser reflected off the gold mirror. At low fluences, a dip, $\Delta R < 0$, is seen around 682 nm, which most likely arises from the induced one-exciton to two-exciton transitions in individual J-aggregate domains.[25,29] The excited-state absorption band is blue-shifted by about 10 nm with respect to the one-exciton resonance (see supporting online material). At higher fluences, it is apparently bleached as well and ΔR changes sign at the highest F_{pu}, reflecting the complex interplay between exciton relaxation, dissociation, and exciton−exciton annihilation dynamics.[25]

LINEAR OPTICAL RESPONSE OF THE HYBRID NANOSTRUCTURES

For our grating structures, we have chosen a narrow slit width of ~45 nm and a shallow depth of ~30 nm to ensure narrow SPP resonances.[30] When such gratings, coated with a dye-containing polymer film, are illuminated with p-polarized light at incidence angle θ, evanescent SPP fields are excited at the

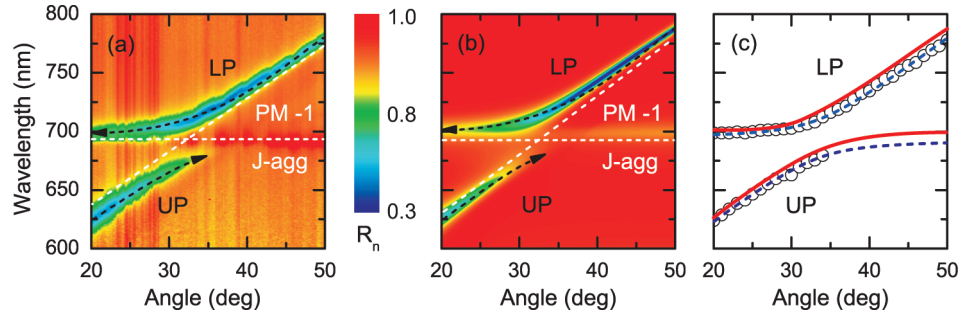

Figure 2. (a) Angle-resolved normalized *p*-polarized reflectivity $R_n = R_h/R_d$ spectra obtained at $T = 77$ K by dividing the reflectivity R_h of the hybrid nanostructure with $a_0 = 430$ nm by that of a J-aggregate layer deposited on a planar gold film, R_d (see Supporting Information). This normalization emphasizes the strong coupling between J-aggregate excitons and PM[−1] SPP with a large $\Omega_R \sim 55$ meV. The white and black dashed lines indicate the dispersion of the uncoupled and coupled resonances, respectively. (b) Calculated *p*-polarized reflection spectra obtained by solving Maxwell's equations. (c) Comparison of the polariton dispersion obtained from observed spectra (open circles), Maxwell's equations (solid line), and coupled-oscillator model (dashed line).

polymer−metal (PM) interface by transferring momentum $n(2\pi)/(a_0)$, $n \in \mathbf{Z}$, to the incident photons. Small grating periods are chosen to only excite the PM[$n = -1$] SPP and to avoid interactions among different SPP modes.[31] For the $a_0 = 430$ nm sample, the PM[−1] resonance energy can be varied between 630 and 780 nm and, hence, can be tuned into resonance with the J-aggregate excitons by varying θ between 20 and 50°. Figure 1d illustrates the electric component of the SPP fields, that is, $|\vec{E}(x, z)|$, obtained from a full solution of Maxwell's equations for our nanostructure for monochromatic, *p*-polarized plane-wave illumination at $\theta = 32°$, corresponding to the exciton−SPP resonance. The calculations reveal strong evanescent SPP fields localized mainly near the slit region and characterized by a short decay length well below 100 nm.

We now discuss the linear reflectivity spectra of a J-aggregated cyanine dye film deposited on such a grating (Figure 2). The hybrid nanostructure reflectivity, R_h spectra show again a strong reflectivity dip at the exciton resonance, only faintly reduced compared to that of R_d. In addition, new and pronounced dips in reflectivity arise since the incident photons can now also couple to SPP excitations of the grating (see Supporting Information). To emphasize the polariton response, normalized angle-resolved reflectivity spectra $R_n = R_h/R_d$ are shown in Figure 2a. A clear anticrossing of the polariton-related dips in reflectivity is observed. This anticrossing is a signature of the strong coupling between excitons and SPPs in the hybrid structure. The interaction between the excitonic transition dipole moment density $\vec{\mu}_X(\vec{r})$ and the local SPP field $\vec{E}_{SPP}(\vec{r})$ induces an exciton-SPP coupling with Rabi energy Ω_R. This results in the formation of two coupled modes, the upper (UP) and the lower (LP) exciton-SPP-polariton modes (excimons) with eigenenergies

$$\tilde{\omega}_{UP,LP} = \frac{1}{2}(\tilde{\omega}_X + \tilde{\omega}_{SPP}) \pm \sqrt{\frac{1}{4}(\tilde{\omega}_X - \tilde{\omega}_{SPP})^2 + \Omega_R^2} \quad (1)$$

where $\tilde{\omega}_{X,SPP} = \omega_{X,SPP} - i\gamma_{X,SPP}$ denote the (complex) eigenenergies of the uncoupled exciton and SPP, respectively. Under our experimental conditions, we observe no effect of the laser intensity on the polariton resonance energies. We therefore conclude that Ω_R, which scales as $\Omega_R \propto (1 + N)^{1/2}$, N being the number of photons per SPP mode,[32] is mainly governed by the coupling of the exciton dipoles to the vacuum SPP field E^0_{SPP}, whose field strength apparently exceeds that induced by the external laser field. Therefore, $E_{SPP} \simeq E^0_{SPP}$ and the external laser field does not affect the linear spectra.

The results in Figure 2a are qualitatively well reproduced by a numerical solution of Maxwell's equation for this hybrid structure [Figure 2b]. Here, we take a Lorentzian oscillator model for the dye response and a constant background dielectric function ε_{bg} to account for the polymer film. These calculations give clear evidence for the formation of the coupled exciton−SPP modes. The dispersion relations of the UP (higher energy) and LP (lower energy) polariton modes [Figure 2c] are readily derived from the reflectivity dips in Figure 2a,b and agree well with the predictions of eq 1 for $\Omega_R \sim 55$ meV. This value of Ω_R is somewhat smaller than those reported in earlier studies[6,7,19,27,28] because we used thinner dye films and narrow, shallow gratings to minimize radiative SPP damping[30,31] and to increase the polariton lifetime.

NONLINEAR OPTICAL RESPONSE OF THE HYBRID NANOSTRUCTURES

We now turn to the nonlinear optical properties of our hybrid structures. Experimentally, we illuminate the sample at normal incidence with a short, 80 fs, off-resonant *p*-polarized pump laser pulse centered at 620 nm. The pump laser excites J-aggregate excitons in the tail of their absorption spectrum [Figure 1b], yet does not couple to SPPs throughout the entire range of incidence angles studied here. Therefore, we expect that it will mainly alter the exciton density n_X in the J-aggregate film on an ultrafast time scale. The experi-

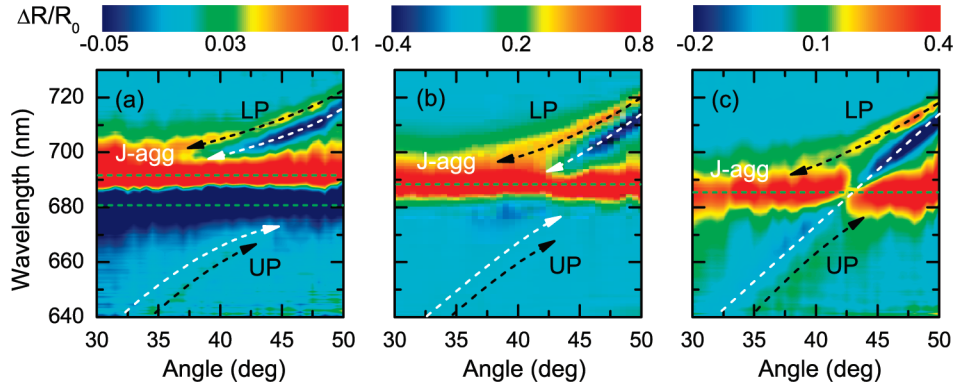

Figure 3. Angle-resolved $\Delta R/R_0$ spectra ($T = 77$ K) of the hybrid structure with a grating period of $a_0 = 380$ nm. The sample is excited by 80 fs pulses centered at 620 nm. The spectra are recorded in a nearly collinear pump−probe setup at a delay of 150 fs. Results are presented for pump energies of (a) 1.4, (b) 7, and (c) 25 nJ, which correspond to fluences of $F_{pu} = 9$, 44, and 159 μJ/cm^2, respectively. All panels show (i) the angle-dependent nonlinear exciton-SPP polariton response (white dashed lines), (ii) the polariton features of the linear spectra (black dashed lines), and (iii) the angle-independent nonlinear response of the J-aggregate (green dashed lines).

ments aim at probing the effect of this change in n_X on the optical properties of the hybrid structure. We achieve this by monitoring the pump-induced changes in the reflectivity ΔR of a weak broad-band *p*-polarized probe pulse incident at angle θ in a nearly collinear pump−probe setup.

Angle-resolved $\Delta R/R_0$ spectra recorded at a delay $\Delta t = 150$ fs for a J-aggregate film on a gold grating with a period of $a_0 = 380$ nm are shown in Figure 3 for three different pump fluences. In all the experiments, we see a pronounced and angle-independent optical nonlinearity near the exciton resonance. The pump fluence dependence of its line shape principally follows that discussed in Figure 1c. These signatures reflect the optical nonlinearities of those excitons, which are not strongly coupled to the SPP field and are therefore similar to those seen for a J-aggregate film deposited on planar metal.

More important is the similarly pronounced nonlinearity near the polariton resonance energies. It is significant even at 30 nm wavelength difference and at incidence angles which differ up to about 10° from the exciton−SPP crossing. This is rather remarkable and clearly demonstrates that the strong coupling between exciton and SPP mode transfers excitonic nonlinearity to the new coupled resonances. In contrast to the absorptive shape of the linear R_n spectrum in Figure 2 with a minimum at $\omega = \omega_{UP,LP}$, the polariton nonlinearity ΔR exhibits a dispersive line shape at all pump fluences and incidence angles. A detailed analysis shows that the positive $\Delta R > 0$ peak (marked by black lines in Figure 3), that is, an increase in probe reflectivity, is found slightly ($\simeq$5−10 meV) above (UP branch) or slightly below (LP branch) the polariton resonance energies $\omega_{UP,LP}$ (see Supporting Information). A minimum in ΔR (marked by the white dashed lines in Figure 3) is always found on the low-energy (UP) or high-energy (LP) side of $\omega_{UP,LP}$. In the nonlinear spectra in Figure 3, the magnitude of the signal from the UP branch is generally somewhat smaller than anticipated from the linear spectra shown in Figure 2. It is expected that the UP nonlinear signal is lower than that of the LP branch. The increase in radiative broadening of the UP resonance with decreasing wavelength[30] results in a somewhat broader linewidth of the UP branch. Since the shift in Rabi frequency is the same for UP and LP branch, the magnitude of the UP nonlinearity is therefore reduced. This argument is only valid in the limit of a shift in Rabi frequency which is much smaller than the linewidth. Indeed, the relative strength of the UP nonlinearity increases at higher fluences.

EFFECT OF EXCITON DENSITY ON EXCITON−SPP POLARITON FORMATION

To explain the observed spectral line shape of the nonlinear spectrum, we consider the effect of the off-resonant pump on Ω_R. The pump-generated exciton density n_X will saturate the excitonic oscillator strength which, in thermal quasi-equilibrium, may be approximated as $f = f_0/[1 + (n_X/n_S)]$.[33] Here, f_0 denotes the excitonic oscillator strength in the linear regime in the absence of the pump and n_S, the exciton saturation density. This accordingly reduces the exciton transition dipole density $\mu_X \propto \sqrt{f}$. The saturation of those excitons $n_{X,c}$ that couple strongly to the SPP field will therefore induce a reduction in the splitting $\Omega_R = \Omega_{R,0}/[1 + (n_{X,c}/n_S)]^{1/2}$, where $\Omega_{R,0}$ is the Rabi energy in the absence of a pump. A similar bleaching of Rabi splitting has been seen in earlier stationary and time-resolved measurements on semiconductor microcavities.[34,35] Here, it is observed for the first time in a hybrid metal−molecular aggregate nanostructure.

The pump-induced change in Ω_R qualitatively explains the observed ΔR signatures. On the LP branch, the pump will transiently shift the polariton resonance to higher energies, eq 1, resulting in a dispersive ΔR resonance with a positive peak at lower energies. On the UP branch, the energy shift is in the opposite direc-

tion. This indicates that the dip in reflectivity (white dashed lines in Figure 3) probes the polariton resonance energies $\omega_{UP,LP}$ in the presence of the pump. At the highest fluence, Figure 3c, the angle-dependence of the dip principally follows the dispersion relation of the uncoupled SPP mode of the nanoslit array, suggesting that Ω_R has been reduced close to zero.

To quantify the effect of the exciton saturation on Ω_R, we have plotted in Figure 4 the resonance energies of (a) the $\Delta R > 0$ peak and (b−d) the dips $\Delta R < 0$ at the three pump fluences of Figure 3 as open circles. Because the $\Delta R > 0$ peak reflects the linear reflectivity in the absence of the pump pulse, it is independent of the fluence, whereas the $\Delta R < 0$ dip is fluence-dependent. The data are compared to the same quantities deduced from a full solution of Maxwell's equation (solid lines) and from the coupled oscillator model (dashed lines). The data in (a) confirm Ω_R of ~60 meV in the absence of the pump. The data in (b−d) indicate a reduction in Ω_R to 20 (b), 5 (c), and 0 meV (d) with increasing power. These results support the conclusion that most of the strong polariton nonlinearities seen in Figure 3 result from a saturation of Ω_R. A more quantitative analysis of the pump effect on Ω_R should therefore be based on eq 1 together with an appropriate line shape model for the polariton resonances. For low pump fluences, such an analysis suggests smaller changes in Ω_R, specifically a transient reduction by 5 meV at 9 μJ/cm^2.

The effects of the pump-induced saturation of Ω_R on the optical properties of the hybrid structures are rather remarkable. Figure 5a shows the probe reflectivity spectra recorded at $\theta = 49°$ in the absence and presence of a pump at $F_{pu} = 44$ μJ/cm^2, preceding the probe pulse by 150 fs. As highlighted in Figure 5a, the pump-induced exciton creation reduces the sample reflectivity in the shaded area by up to 40%, *e.g.*, from 80% down to 46% at 710 nm. The exciton creation shifts the LP resonance energy ω_{LP} by 11 meV, slightly more than the line width $\gamma_{LP} = 10$ meV of the resonance (see Figure 3a). In principle, even larger shifts are expected for higher fluences. Data at intermediate fluences are chosen in Figure 5a to definitely ensure that the observed shifts are unaffected by possible long-term photobleaching of J-aggregated dyes. Such a pronounced shift of the polariton resonance is substantially different from the reduction in polariton peak height with small change in Rabi splitting observed in experiments on high-quality semiconductor microcavities, where excitation-induced dephasing effects are important.[36] The change in reflectivity around 690 nm is more complex since it results from both the bleaching of uncoupled excitons and the red-shift of ω_{UP}.

Figure 5b compares the time dynamics of the normalized $\Delta R/R_0$ signal at the bare exciton, and the upper and the lower polariton resonances. The data are recorded at $\theta = 42.5°$ and for $F_{pu} = 159$ μJ/cm^2, where

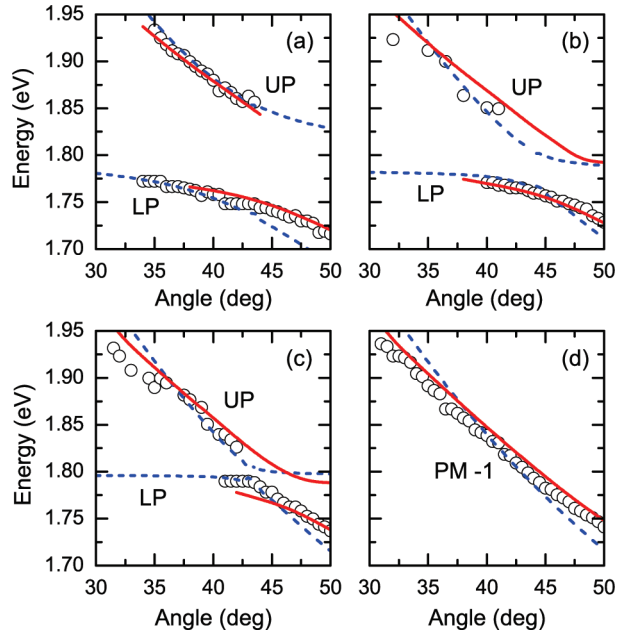

Figure 4. UP and LP resonance energies deduced from the nonlinear spectra (Figure 3) by taking (a) the positive peak of the $\Delta R/R_0$ signal at 9 μJ/cm^2 and its negative peak at (b) 9, (c) 44, and (d) 159 μJ/cm^2. Open circles are deduced from the experimental data, and solid and dashed lines represent the same quantities extracted from the full solution of Maxwell's equations and from the coupled-oscillator model, respectively. The coupling parameter Ω_R in the oscillator model decreases from 60 to 20, 5, and 0 meV with increasing pump fluence.

all three resonances are spectrally well separated. The dynamics at a probe wavelength of 685 nm reveal an exciton lifetime of less than 0.9 ps, typical for this kind of J-aggregated dye whereas the polariton lifetimes are substantially shorter, less than 0.4 ps. Such a reduction of the polariton lifetimes in comparison to those of the uncoupled excitons may to some extent be expected due to the very strong radiative damping of SPP modes (their lifetimes are only in the range of a few tens of fs).[30,31] The enhanced radiative damping of the polariton modes may therefore be the reason for the reduced lifetimes of the UP and LP modes. Our present measure-

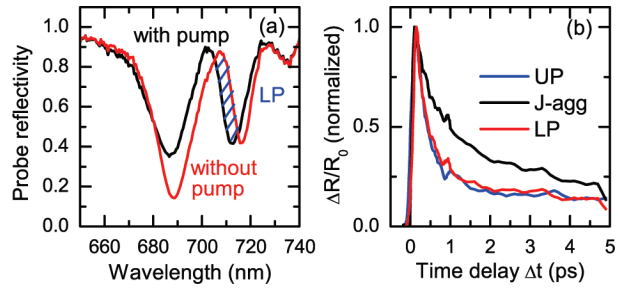

Figure 5. (a) Probe reflectivity of the hybrid structure at $\theta = 49°$ in the absence (black) and presence (red) of a pump, recorded at $\Delta t = 150$ fs and for $F_{pu} = 44$ μJ/cm^2. The pump-induced reduction of Ω_R spectrally shifts the LP resonance and strongly reduces the reflectivity around 710 nm, making the sample essentially a switchable mirror. (b) Time dynamics of the normalized $\Delta R/R_0$ signal at the UP (675 nm), LP (710 nm), and exciton (685 nm) resonances at $\theta = 42.5°$ and $F_{pu} = 159$ μJ/cm^2. The short UP and LP lifetimes reflect the pronounced radiative polariton damping.

ments, however, have been performed with nonresonant pumping resulting in the creation of a broad distribution of both uncoupled and coupled excitons. The dynamics measured in Figure 5b therefore do not necessarily probe the radiative damping dynamics but rather a complex interplay between exciton relaxation and radiative damping dynamics. For a more direct analysis of the radiative polariton damping, experiments under resonant excitation conditions are needed which are currently underway in our laboratory. In Figure 5b, the transient change in reflectivity vanishes almost completely (>75%) within 1 ps. This shows that the pump-induced change in Ω_R and hence the sample reflectivity is fully reversible occurring on a very fast time scale.

The observation of such a pronounced, externally induced, fast and reversible change in reflectivity of a metal-molecular aggregate nanostructure suggests that these hybrid structures can indeed act and potentially find applications as externally controllable, ultrafast switchable mirrors. For future applications it is certainly necessary to use active materials which are less susceptible to photodamage.[37] It also should be interesting to further miniaturize the photonic cavity volume to approach the fundamental limit of an ultrafast single photon transistor.[23]

CONCLUSIONS

We investigated the ultrafast optical nonlinearities of a prototypical metal−molecular aggregate hybrid nanostructure. We show that the optical properties of such hybrid structures are governed by the strong coupling between excitons and SPPs and demonstrate a reversible transition between the strong and weak coupling regime on a subpicosecond time scale. This allows us to transiently reduce the reflectivity of a gold mirror by up to 40% in a range of near-infrared wavelengths. We anticipate that such a strong, externally controllable exciton−plasmon interaction is of considerable importance for implementing novel nanophotonic devices such as switches, modulators, or transistors, potentially operating on ultrafast time scales and with only a single photon thus adding an important active functionality to high speed, high density plasmonic circuits.

EXPERIMENTAL SECTION

All the experiments are performed using an angle-resolved reflectivity setup with angular resolution of 0.2° and spectral resolution of 0.2 nm. A coherent white-light source (Fianium SC-450-4) is used for linear reflectivity measurements recorded with *p*-polarized light, whereas $\Delta R/R_0$ measurements are performed using a pump−probe setup based on an optical parametric amplifier system operating at a repetition rate of 1 kHz. Pump pulses (80-fs) centered at 620 nm are used for excitation and a white-light continuum generated in a sapphire plate provides time-delayed probe pulses covering the range from 630 to 750 nm. Both pump and probe pulses are *p*-polarized and nearly collinearly focused onto the sample with a beam diameter of ~100 μm at an incidence angle θ with respect to the sample normal. Angle-resolved $\Delta R/R_0$ spectra from 30 to 50° are recorded at different pump−probe delays Δt under vacuum at a temperature of $T = 77$ K to minimize J-aggregate photobleaching. Control experiments are performed on a planar dye-coated gold sample without nanoslit arrays.

Acknowledgment. We thank the Deutsche Forschungsgemeinschaft (SPP 1391), European Community (FP-7-INFRASTRUCTURES-2008-1, "Laserlab Europe II", Contract No. 228334) and the Korea Foundation for International Cooperation of Science and Technology (Global Research Laboratory Project, K20815000003) for financial support.

Supporting Information Available: Angle-dependent reflectivity spectra of the J-aggregated dye film deposited on a bare gold film and on a gold nanoslit array. This material is available free of charge *via* the Internet at http://pubs.acs.org.

REFERENCES AND NOTES

1. Akimov, A. V.; Mukherjee, A.; Yu, C. L.; Chang, D. E.; Zibrov, A. S.; Hemmer, P. R.; Park, H.; Lukin, M. D. Generation of Single Optical Plasmons in Metallic Nanowires Coupled to Quantum Dots. *Nature* **2007**, *450*, 402–406.
2. Oulton, R. F.; Sorger, V. J.; Zentgraf, T.; Min, R. M.; Gladden, C.; Dai, L.; Bartal, G.; Zhang, X. Plasmon Lasers at Deep Subwavelength Scale. *Nature* **2009**, *461*, 629–632.
3. Vasa, P.; Lienau, C. An Unusual Marriage: Coupling Molecular Excitons to Surface Plasmon Polaritons in Metal Nanostructures. *Angew. Chem., Int. Ed.* **2010**, *49*, 2476–2477.
4. Salomon, A.; Genet, C.; Ebbesen, T. W. Molecule-Light Complex: Dynamics of Hybrid Molecule-Surface Plasmon States. *Angew. Chem., Int. Ed.* **2009**, *48*, 8748–8751.
5. Pockrand, I.; Brillante, A.; Möbius, D. Exciton-Surface Plasmon Coupling: An Experimental Investigation. *J. Chem. Phys.* **1982**, *77*, 6289–6295.
6. Bellessa, J.; Bonnand, C.; Plenet, J. C.; Mugnier, J. Strong Coupling between Surface Plasmons and Excitons in an Organic Semiconductor. *Phys. Rev. Lett.* **2004**, *93*, 036404.
7. Dintinger, J.; Klein, S.; Bustos, F.; Barnes, W. L.; Ebbesen, T. W. Strong Coupling between Surface Plasmon Polaritons and Organic Molecules in Subwavelength Hole Arrays. *Phys. Rev. B* **2005**, *71*, 035424.
8. Hakala, T. K.; Toppari, J. J.; Kuzyk, A.; Pettersson, M.; Tikkanen, H.; Kunttu, H.; Torma, P. Vacuum Rabi Splitting and Strong-Coupling Dynamics for Surface Plasmon Polaritons and Rhodamine 6G Molecules. *Phys. Rev. Lett.* **2009**, *103*, 053602.
9. Gomez, D. E.; Vernon, K. C.; Mulvaney, P.; Davis, T. J. Surface Plasmon Mediated Strong Exciton-Photon Coupling in Semiconductor Nanocrystals. *Nano Lett.* **2010**, *10*, 274–278.
10. Vasa, P.; et al. Coherent Exciton-Surface-Plasmon-Polariton Interaction in Hybrid Metal-Semiconductor Nanostructures. *Phys. Rev. Lett.* **2008**, *101*, 116801.
11. Thompson, R. J.; Rempe, G.; Kimble, H. J. Observation of Normal-Mode Splitting for an Atom in an Optical Cavity. *Phys. Rev. Lett.* **1992**, *68*, 1132–1136.
12. Weisbuch, C.; Nishioka, M.; Ishikawa, A.; Arakawa, Y. Observation of the Coupled Exciton- Photon Mode Splitting in a Semiconductor Quantum Microcavity. *Phys. Rev. Lett.* **1992**, *69*, 3314–3317.
13. Lidzey, D. G.; Bradley, D. D. C.; Virgili, T.; Armitage, A.; Skolnick, M. S.; Walker, S. Room Temperature Polariton Emission from Strongly Coupled Organic Semiconductor Microcavities. *Phys. Rev. Lett.* **1999**, *82*, 3316–3319.
14. Lidzey, D. G.; Bradley, D. D. C.; Armitage, A.; Walker, S.; Skolnick, M. S. Photon-Mediated Hybridization of Frenkel Excitons in Organic Semiconductor Microcavities. *Science* **2000**, *288*, 1620–1623.

15. Saba, M.; et al. High-Temperature Ultrafast Polariton Parametric Amplification in Semiconductor Microcavities. *Nature* **2001**, *414*, 731–735.
16. Christopoulos, S.; et al. Room-Temperature Polariton Lasing in Semiconductor Microcavities. *Phys. Rev. Lett.* **2007**, *98*, 126405.
17. Deng, H.; Weihs, G.; Santori, C.; Bloch, J.; Yamamoto, Y. Condensation of Semiconductor Microcavity Exciton Polaritons. *Science* **2002**, *298*, 199–202.
18. Kasprzak, J.; et al. Bose-Einstein Condensation of Exciton Polaritons. *Nature* **2006**, *443*, 409–414.
19. Bellessa, J.; et al. Giant Rabi Splitting Between Localized Mixed Plasmon-Exciton States in a Two-Dimensional Array of Nanosize Metallic Disks in an Organic Semiconductor. *Phys. Rev. B* **2009**, *80*, 033303.
20. Dintinger, J.; Robel, I.; Kamat, P.; Genet, C.; Ebbesen, T. Terahertz All-Optical Molecule- Plasmon Modulation. *Adv. Mater.* **2006**, *18*, 1645–1648.
21. Wiederrecht, G. P.; Hall, J. E.; Bouhelier, A. Control of Molecular Energy Redistribution Pathways *via* Surface Plasmon Gating. *Phys. Rev. Lett.* **2007**, *98*, 083001.
22. Zheludev, N. I.; Provirnin, S. L.; Papasimakis, N.; Fedotov, V. A. Lasing Spaser. *Nat. Photonics* **2008**, *2*, 351–354.
23. Chang, D. E.; Sorensen, A. S.; Demler, E. A.; Lukin, M. D. A Single-Photon Transistor Using Nanoscale Surface Plasmons. *Nat. Phys.* **2007**, *3*, 807–812.
24. Kobayashi, T., Ed. *J-Aggregates*; World Scientific: Hackensack, NJ, 1996.
25. van Burgel, M.; Wiersma, D. A.; Duppen, K. The Dynamics of One-Dimensional Excitons in Liquids. *J. Chem. Phys.* **1995**, *102*, 20–33.
26. Michetti, P.; Rocca, G. L. Exciton-Phonon Scattering and Photoexcitation Dynamics in J-Aggregate Microcavities. *Phys. Rev. B* **2009**, *79*, 035325.
27. Wurtz, G. A.; Evans, P. R.; Hendren, W.; Atkinson, R.; Dickson, W.; Pollard, R. J.; Zayats, A. V.; Harrison, W.; Bower, C. Molecular Plasmonics with Tunable Exciton-Plasmon Coupling Strength in J-Aggregate Hybridized Au Nanorod Assemblies. *Nano Lett.* **2007**, *7*, 1297–1303.
28. Fofang, N. T.; Park, T. H.; Neumann, O.; Mirin, N. A.; Nordlander, P.; Halas, N. Plexcitonic Nanoparticles: Plasmon-Exciton Coupling in Nanoshell-J-Aggregate Complexes. *Nano Lett.* **2008**, *8*, 3481–3487.
29. Fidder, H.; Knoester, J.; Wiersma, D. A. Observation of the One-Exciton to Two-Exciton Transition in a J-Aggregate. *J. Chem. Phys.* **1993**, *98*, 6564–6566.
30. Kim, D. S.; Hohng, S. C.; Malyarchuk, V.; Yoon, Y. C.; Ahn, Y. H.; Yee, K. J.; Park, J. W.; Kim, J.; Park, Q. H.; Lienau, C. Microscopic Origin of Surface-Plasmon Radiation in Plasmonic Band-Gap Nanostructures. *Phys. Rev. Lett.* **2003**, *91*, 143901.
31. Ropers, C.; Park, D. J.; Stibenz, G.; Steinmeyer, G.; Kim, J.; Kim, D. S.; Lienau, C. Femtosecond Light Transmission and Subradiant Damping in Plasmonic Crystals. *Phys. Rev. Lett.* **2005**, *94*, 113901.
32. Sanchez-Mondragon, J. J.; Narozhny, N. B.; Eberly, J. H. Theory of Spontaneous-Emission Line Shape in an Ideal Cavity. *Phys. Rev. Lett.* **1983**, *51*, 550–553.
33. Khitrova, G.; Gibbs, H. M.; Jahnke, F.; Kira, M.; Koch, S. W. Nonlinear Optics of Normal-Mode-Coupling Semiconductor Microcavities. *Rev. Mod. Phys* **1999**, *71*, 1591–1639.
34. Houdré, R.; Gibernon, J. L.; Pellandini, P.; Stanley, R. P.; Oesterle, U.; Weisbuch, C.; O'Gorman, J.; Roycroft, B.; Ilegems, M. Saturation of the Strong-Coupling Regime in a Semiconductor Microcavity: Free-Carrier Bleaching of Cavity Polaritons. *Phys. Rev. B* **1995**, *52*, 7810–7813.
35. Rhee, J.; Citrin, D.; Norris, T.; Arakawa, Y.; Nishioka, M. Femtosecond Dynamics of Semiconductor Microcavity Polaritons in the Nonlinear Regime. *Solid State Commun.* **1996**, *97*, 941–946.
36. Jahnke, F.; et al. Excitonic Nonlinearities of Semiconductor Microcavities in the Nonperturbative Regime. *Phys. Rev. Lett.* **1996**, *77*, 5257–5260.
37. Wenus, J.; Ceccarelli, S.; Lidzey, D.; Tolmachev, A.; Slominski, J.; Bricks, J. Optical Strong Coupling in Microcavities Containing J-Aggregates Absorbing in Near-Infrared Spectral Range. *Org. Electron.* **2007**, *8*, 120–126.